

COSMIC RAY

PHYSICS DEGREE Academic Year 2021-2022

Group 17, cohort 3

Rachele Cicioni

Maria Sharon Di Spena

Giacomo Guastella

November 20, 2021

Abstract

The aim of this experiment is to observe the muon component of cosmic rays incident on the Earth's surface and to verify the experimental law followed by their angular distribution at sea level. In order to do this, a calibration procedure of the experimental setup is followed, and the efficiency of the telescope built for observation is checked.

1 Electronic cabling

The experimental apparatus consists of two plastic scintillators connected, on the left and on the right, by light guides to XP2020 photomultipliers. Below the scintillators are two pairs of trackers. The arrangement of the aforementioned elements is shown in **Figure 1**. The electronic diagram is schematized in **Figure 2**. The abbreviations shown in the legend of **Figure 2** will be used below to recall the various components used. The next paragraph explains the previous steps to the final electronic wiring described in **Paragraph 1.2**. The different signals will be indicated as follows:

- UL = UP LEFT
- UR = UP RIGHT
- UP = UP LEFT.AND.UP RIGHT
- DL = DOWN LEFT
- DR = DOWN RIGHT
- DOWN = DOWN LEFT.AND.DOWN RIGHT

1.1 Preliminary steps

The output of the PMT UR is connected to the oscilloscope and the signal characteristics shown in **Table 1** are recorded: Fall time, Rise time, Vmax and Noise level. The error on time measurements is 2 ns because the time measurement was taken using the two oscilloscope cursors appropriately positioned. Each cursor has a sensitivity of 1 ns, and considering the time interval between the two cursors, the overall error is 2 ns. The error on the measurement of amplitudes is 4 mV as for the same reason as before; each cursor has a sensitivity of 2 mV and so the overall error is 4 mV.

The output of the PMT UR is now connected to the CFTD and the square output signal is observed with the oscilloscope and the width of signal is recorded in **Table 1**.

The output of the CFTD is then connected to the CT and the threshold is appropriately set up to have a counting rate of about 40Hz. The counts reported in the table were taken in 10s.

The same procedure is repeated for the UL signal.

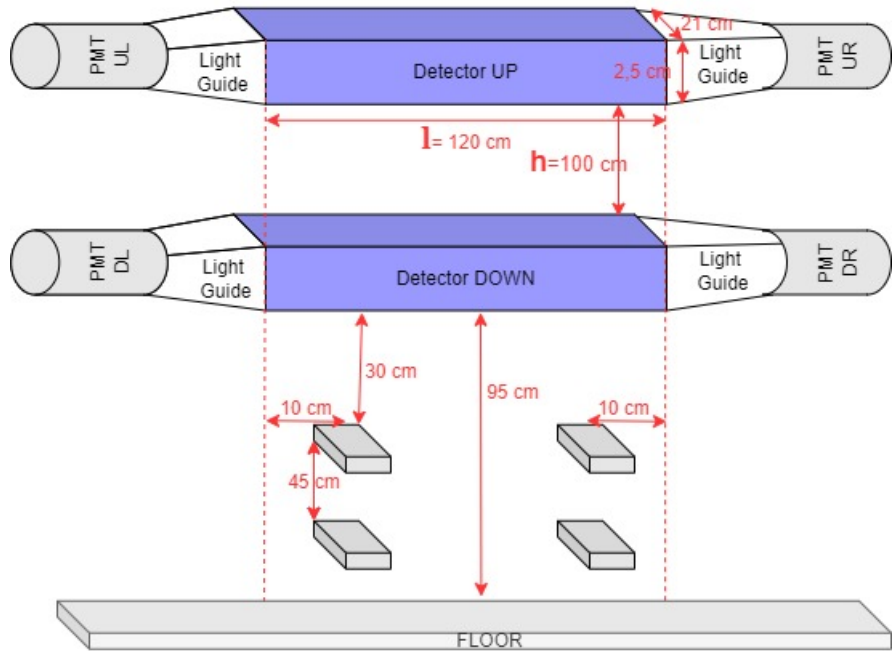


Figure 1: Experimental set-up.

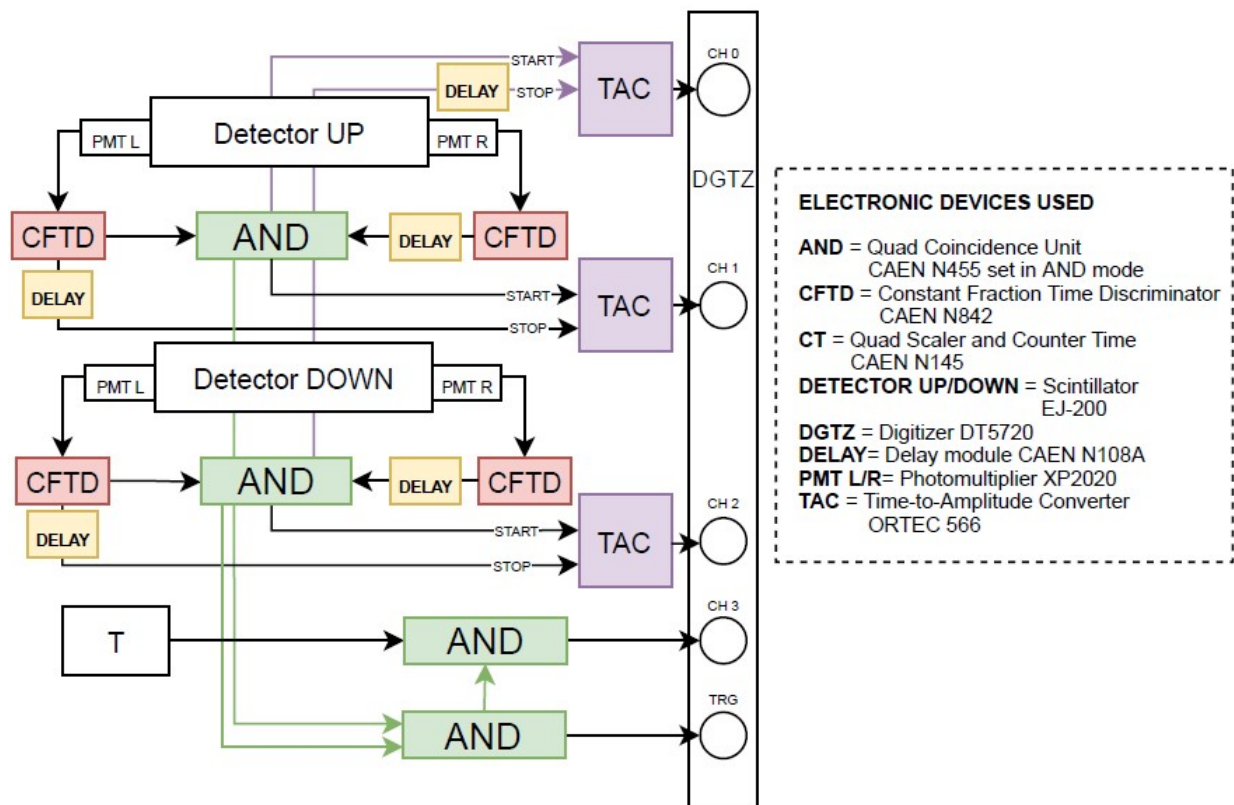


Figure 2: Electronic diagram for the experiment.

	Fall time(ns)	Rise time(ns)	Vmax(mV)	Noise level(mV)	Width(ns)	Counts*	Threshold(mV)
UR	32±2	10±2	120±4	4±4	100±2	432±20	130±1
UL	30±2	9±2	166±4	3±4	100±2	424±21	175±1
DR	42±2	9±2	312±4	4±4	107±2	407±20	130±1
DL	56±2	7±2	213±4	4±4	102±2	420±21	115±1

Table 1: Characterization of the signals UR, UL, DR, DL. *) Counts in 10s.

1.2 Experimental wiring

The outputs of CFTD UR and UL signals are observed with the oscilloscope to check for the overlap. The UR signal is connected to the DELAY and a delay D1 is set with DELAY switches. For a further check, the delay D1 is measured and recorded by connecting the UL and UR-delayed signals to the oscilloscope. All values of delays are recorded in **Table 2**. The UP signal is constructed by inserting the UL and UR-delayed signals in AND. The UL and UP signals are connected to the oscilloscope by measuring the delay D1+D2, where D2 is a delay due to the electronic apparatus. The UP signal is connected to the CT and the counting rate is recorded. The counts in 10s for the signal UP are (336±18)counts. The counts in 10s for the following signal DOWN are (374±19)counts.

We proceed to the wiring for the TAC. The UL (STOP of the TAC) signal is delayed via the DELAY by setting a delay of 48 ns with DELAY switches (the same delay will be set for the DL signal). The UL-delayed signal and the UP signal are connected to the oscilloscope to check and measure the delay. Once there is a sufficient delay between the two signals, the UP signal is connected to the START, the UL-delayed signal to the STOP. Finally, the TAC output signal and the UP signal are connected to the oscilloscope: we check for the presence of the TAC signal for each UP peak.

The entire procedure is repeated for the DOWN detector.

Once the UP and DOWN signals have been implemented, we proceed with the wiring for the UP.AND.DOWN signal, connecting the UP and DOWN signals to the AND. We observe with the oscilloscope a square signal of width (20±4)mV. The DOWN signal is connected to the DELAY by setting a delay of 10 ns. The DOWN-delayed signal (STOP of the TAC) and the UP signal (START of the TAC) are connected to the oscilloscope and a delay between the two signal of (30±2)ns is measured.

At last the signal UP.AND.DOWN.AND.T is implemented with the last AND gate available. The signal T is the T1.OR.T2 signal, where T1 and T2 are the signals of the two pairs of trackers. To complete the wiring of the device, connect the various channels of the DGTZ as follows:

- CH 0: TAC UP.AND.DOWN
- CH 1: TAC UP
- CH 2: TAC DOWN
- CH 3: UP.AND.DOWN.AND.T signal
- TRG: UP.AND.DOWN signal

	D1 set* (ns)	D1 measured** (ns)	D1+D2 measured** (ns)	Delay start/stop*** (ns)
UP	10	11±2	36±2	33±2
DOWN	8	11±2	34±2	16±2

Table 2: Delays of the signals. *) Delays set in the delay module for the signals UR and DR. **) Delays measured with the oscilloscope. ***) Delay measured with the oscilloscope between START and STOP of the TACs.

2 Time calibration

We start from the time calibration of TAC UP. We make the switch from AND to OR in CAEN N455, obtaining the signal UL.OR.UR. The UL.OR.UR signal is delayed by the external DELAY. The

Delay (ns)	Channel
2	1840.2 ± 0.6
4	$(25 \pm 2) \cdot 10^2$
8	3920.2 ± 0.6
16	$(673 \pm 2) \cdot 10^1$
20	8112.2 ± 0.6
26	$(1022 \pm 2) \cdot 10^1$
32	12368.2 ± 0.5

Table 3: Data acquired for TAC UP.

$$m = (2.8487 \pm 0.0002) \cdot 10^{-3} \text{ ns/ch}$$

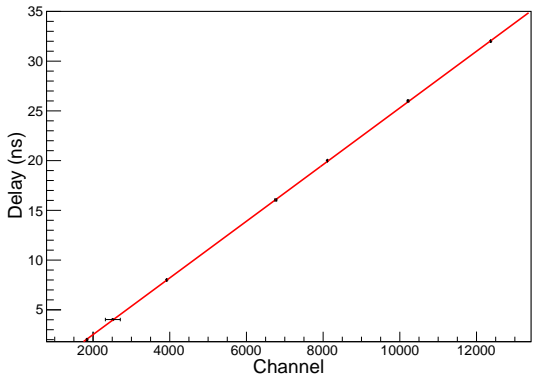


Figure 3: Time calibration TAC UP.

$$q = (-3.188 \pm 0.002) \text{ ns}$$

Delay (ns)	Channel
2	16 ± 8
8	779 ± 6
20	$(289 \pm 2) \cdot 10^1$
26	$(394 \pm 1) \cdot 10^1$
32	5011 ± 2
40	6416.2 ± 0.6
46	7468 ± 6

Table 4: Data acquired for TAC DOWN.

$$m = (5.764 \pm 0.004) \cdot 10^{-3} \text{ ns/ch}$$

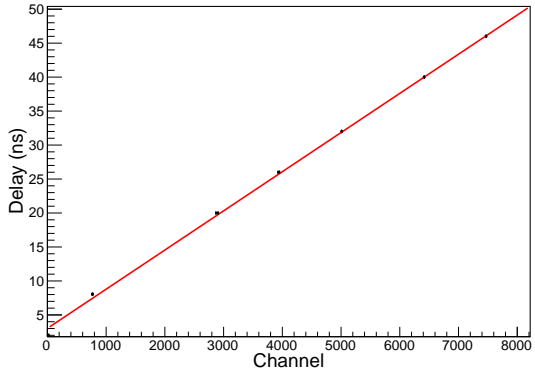


Figure 4: Time calibration TAC DOWN.

$$q = (3.025 \pm 0.003) \text{ ns}$$

Delay (ns)	Channel
2	919 ± 8
4	1238.7 ± 0.3
8	$(19 \pm 2) \cdot 10^2$
16	3180 ± 3
20	$(38 \pm 1) \cdot 10^2$
26	$(478 \pm 1) \cdot 10^1$
32	5771 ± 3

Table 5: Data acquired for TAC UP.AND.DOWN.

$$m = (6.181 \pm 0.004) \cdot 10^{-3} \text{ ns/ch}$$

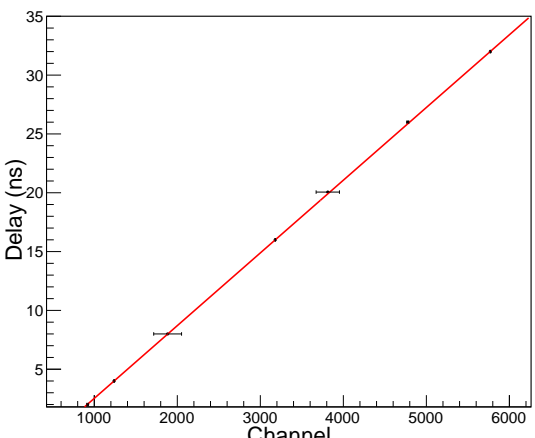


Figure 5: Time calibration TAC UP.AND.DOWN.

$$q = (-3.656 \pm 0.005) \text{ ns}$$

UL.OR.UR signal is the START of the TAC and the UL.OR.UR-delayed signal is the STOP of the TAC, in this way we create a self-coincidence in the TAC. Through the software VERDI, for each delay set in **DELAY**, we record the value of the channels fitting the peak with a gaussian.

The same procedure is performed for TAC DOWN and TAC UP.AND.DOWN.

The **DELAY** values and the channel value acquired in VERDI are shown in **Table 3, 4, 5**. For each TAC we perform a linear fit: $t = m * ch + q$ with the data in the respective table and the line is shown in the figure next to the table. Below the table and the figure there are the values m and q of the linear fit.

3 Position Calibration

With the settings described at the end of **Paragraph 1.2**, a data acquisition of almost 24 hours has been performed, in order to have sufficient statistics. In our case the measurement time is about 22 hours.

The calibration in position for channels 1 and 2 (that correspond to the signals UP and DOWN respectively) is based on the fact that the signals depends only on the time different between left and right. Assuming constant the longitudinal speed of the signals, the difference in time is obviously proportional to the position in which a cosmic ray crosses the scintillator's surface. There is however to consider a constant shift due to the set delays. In order to obtain the calibration in position, it is necessary to know the fixed position that are associated with the measurement of the digitizer (in channels). Therefore, signal in coincidence with the trackers are considered, as they can be considered fixed points due to their small size and their known position in the experimental apparatus (**Figure 1**).

Using a ROOT program, it is possible to consider the events acquired by the UP detector (CH 1) in coinciding with the signals acquired by the UP and DOWN detectors and the trackers (CH 3). These kind of event represents a cosmic ray that reach the scintillator with a vertical trajectory and that pass through the right or left tracker. The same is done for the DOWN detector (CH 2). In this way, two spectra are obtained with two peaks that represent the known trackers position (shown in **Figure 7**). It is possible to obtain the channel-position relation fitting the two peaks with a gaussian in order to obtains the centroids. At the end, the linear relation $pos = m * channel + q$ returns the calibrated spectra (as shown in **Figure 6**) and the results of the analyses are shown in **Table 6**.

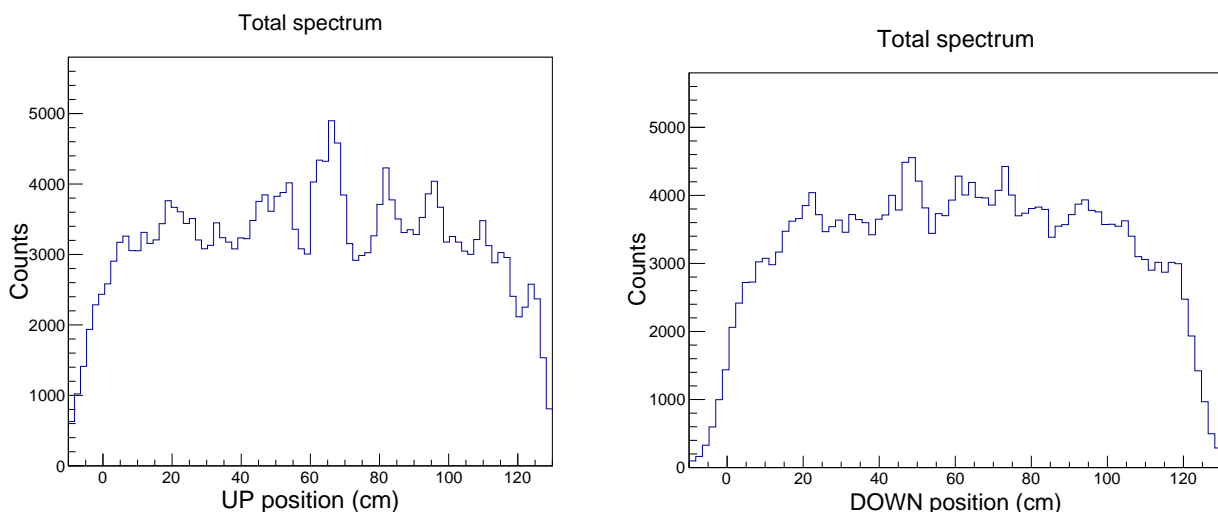


Figure 6: Total spectra of the UP and DOWN detectors calibrated in position.

	Left peak (channel) (10 cm)	Right peak (channel) (110 cm)	m (cm/channel)	q (cm)
UP	5476±13	9260±14	0.0264 ±0.0001	-135±1
DOWN	2179±3	4236±3	0.0486±0.0001	-96±3

Table 6: Linear relation for the calibration in position

The graphs in **Figure 6** shows the spectra obtained by the UP and the DOWN scintillators, calibrated in position. Since the experimental setup is parallel to the Earth' surface, it is expected a uniform distribution of the signals. This trend is confirmed by the graphs, mostly in the center of the apparatus; in facts at the ends of the apparatus fewer signals are acquired, due to ineffective collection.

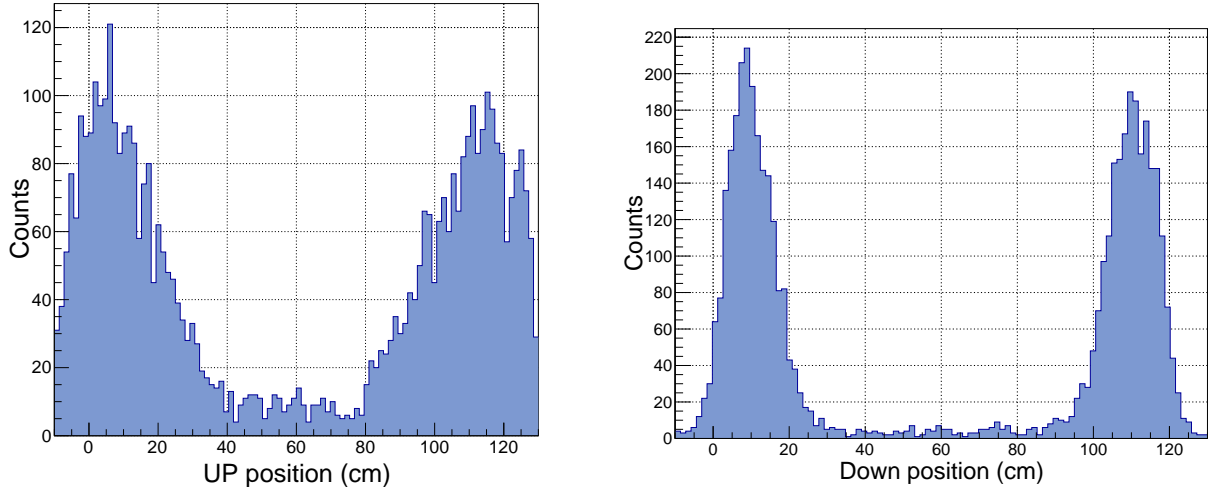


Figure 7: Up and DOWN spectra in coincidence with the trackers

In **Figure 7** is shown the spectra of the UP and DOWN detector respectively obtained by the coincidence with the trackers, already calibrated in position. Can be seen that the DOWN peaks are much narrower than the UP ones. This is probably due to the fact that the DOWN detector is closer to the trackers and therefore the signals acquired in coincidence are found in a smaller spatial region.

4 Correlation between UP and DOWN spectra

Using the events in the "large acquisition file" it is possible to construct the matrix of the position UP versus the position DOWN in order to see the correlation between the two spectra of the two detectors.

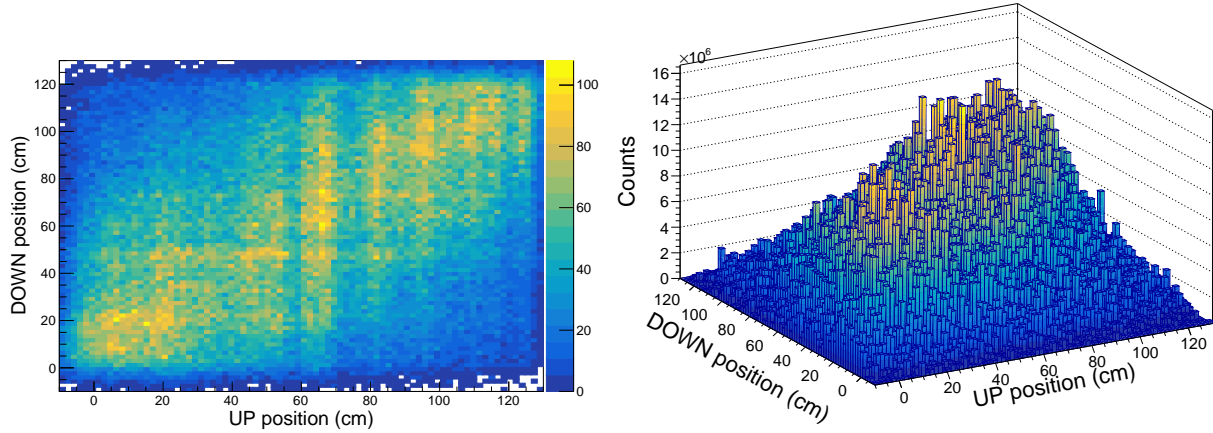


Figure 8: 2D and 3D plots of the correlation between UP and DOWN detectors

As is possible to see in **Figure 8**, there are way more events in the region described by the condition of having the same spatial coordinate in the UP and DOWN detectors. In fact we have more events on the diagonal of the plots. This is in accordance with the theoretical spatial distribution of the cosmic rays ($\propto \cos^2(\theta)$), that predicts vertical trajectories.

It's also interesting to construct the multidimensional plots with also the coincidence with the trackers.

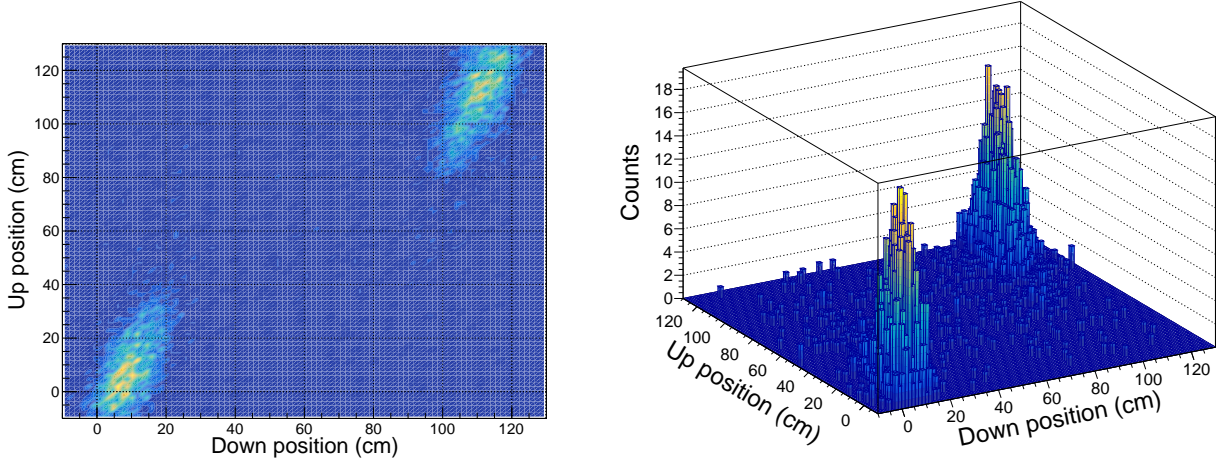


Figure 9: 2D and 3D plots of the correlation between UP and DOWN detectors in coincidence with the trackers

As is shown in **Figure 9** the positions of the two peaks emerge more clearly, and is also possible to observe there is more dispersion in the UP detector than in the DOWN one that confirm what is shown in **Figure 7**.

5 Events at detector's edge

To study in a more detailed way the angular distribution of cosmic rays, it's interesting to analyze the spectrum of the DOWN detector in coincidence with the events acquired in a specific fixed spatial region in the UP detector. In this case, the events in the UP position (x_U = spatial distance from the LEFT edge of the UP detector) $[0, 10]$ cm and $[110, 120]$ cm are studied. As the DOWN position (x_D = spatial distance from the LEFT edge of the DOWN detector) increases, a reduction of the events is expected. This is due to two effects:

- the $\cos^2(\theta)$ dependence of the cosmic rays flux;

- a $\cos(\theta)$ reduction due to the angle with the surface.

Considering a constant efficiency of the scintillator, the total counting should be proportional to the $\cos^3(\theta)$. The angle can be estimated by the geometry of the apparatus: $\cos(\theta) = \frac{h}{\sqrt{h^2+x_D^2}}$, where h is the distance between the UP and the DOWN detector. So the counting is:

$$N(x_D) \propto \left(\frac{h}{\sqrt{h^2+x_D^2}} \right)^3$$

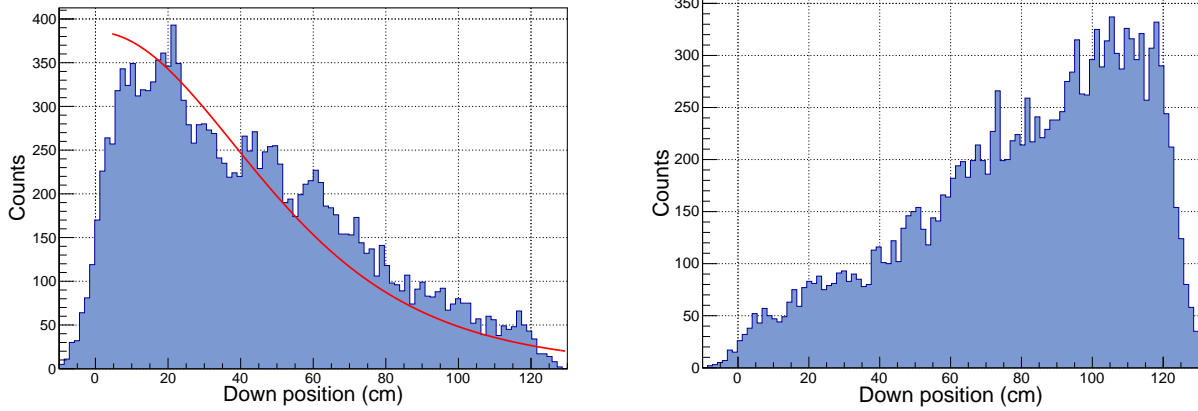


Figure 10: Spectra in the DOWN detectors of cosmic rays which pass through the UP detector in the region $[0, 10]$ cm (left) and $[110, 120]$ cm (right). In red the theoretical expectation.

The decreasing trend of the function is respected, however there is a discrepancy with the theoretical expectation, probably due to the not constant efficiency of the scintillator in function of x_D . It is possible to study the correlation between the restricted DOWN spectra and the time measurement of the UP-AND-DOWN signals acquired by the CH 0 of the digitizer (the TAC signal is already calibrated in time in **Section 2, Figure 5**). Knowing that the energy of a cosmic muon at sea level is about 4GeV, the Lorentz factor γ is about 40, which corresponds to a speed $v_\mu \sim 0.9997c$. For this reason, it's a good approximation to consider that the muons travel at the speed of light. The light inside the detectors in the laboratory however travels at $v = 0.6c$, given the refractive index of the detectors. So is possible to calculate the measured TAC time. Knowing that the TAC signal amplitude is proportional to the difference between the time the signals reaches the UP-RIGHT detector and the DOWN-RIGHT detector, and assuming that the ray hits the UP detector at time $t=0$, the signal should be detected after:

$$t_{UR} = \frac{l - x_U}{v} \quad t_{UL} = \frac{x_U}{v}$$

$$t_{DL} = \frac{\sqrt{h^2 + (x_D - x_U)^2}}{c} + \frac{x_D}{v} \quad t_{DR} = \frac{\sqrt{h^2 + (x_D - x_U)^2}}{c} + \frac{l - x_D}{v}$$

In this way, it is possible to obtain a dependence of the TAC signal on the DOWN position:

$$T_{UD}(x_D) = t_{DR} - t_{UR} + D_{UD} = \frac{\sqrt{h^2 + (x_D - x_U)^2}}{c} + \frac{x_U - x_D}{v} + D_{UD}$$

where D_{UD} is a offset caused by the electronics and the delay on the stop.

Fixing the position $x_U = 5$ cm and $x_U = 115$ cm as we vary where we restrict the UP signal, we have a function of the TAC time as a function of x_D .

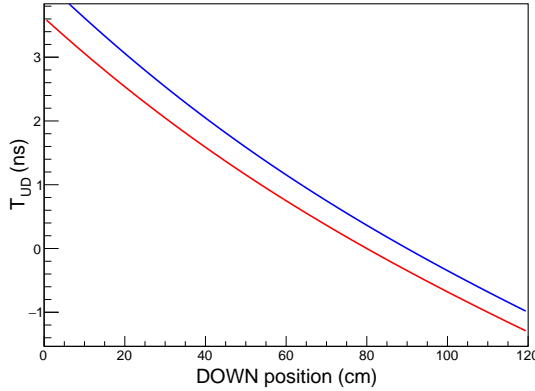


Figure 11: Theoretical expectation of T_{UD} without any delay offset. The red line represent the UP-LEFT restriction trend, the blue line represent the UP-RIGHT restriction trend

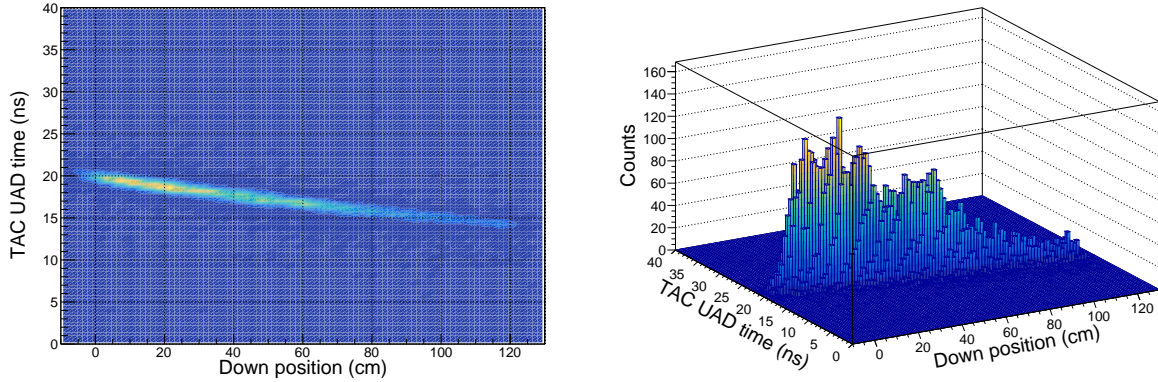


Figure 12: 2D and 3D plots of the correlation between DOWN position with UP-LEFT restriction and TAC UP-AND-DOWN

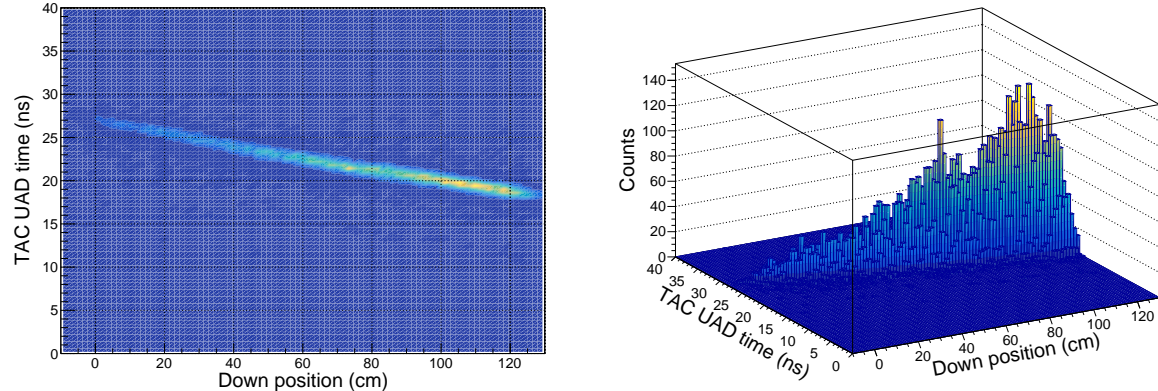


Figure 13: 2D and 3D plots of the correlation between DOWN position with UP-RIGHT restriction and TAC UP-AND-DOWN

The plots of the TAC UP-AND-DOWN in function of the position of the DOWN detector with the restriction at the UP detector edges follows the expected trend shown in **Figure 11**, highlighting a negative correlation.

6 Angular Distribution

An useful measure to investigate the origin of cosmic ray muons is their angular distribution with respect to the Zenith angle. One of the purposes of this experience is to verify the experimental law according to which the incidence rate of the muon component of cosmic rays on the earth's surface at sea level is approximately proportional to the square of the cosine of the angle of incidence:

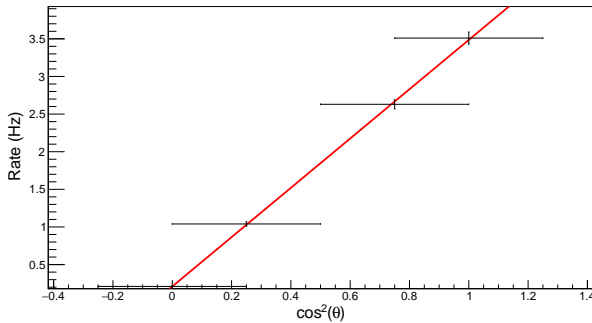
$$R(\theta) = R_0 \cos^2(\theta)$$

For this purpose spectra acquisitions are performed in about 45 minutes using the VERDI software and by varying the angle of the experimental apparatus with respect to the earth's surface. In particular, we carry out measurements at 0° , 30° , 60° and 90° . From these spectra is possible to obtain the count of the events recorded by the scintillators UP and DOWN. Since the counting rates follow a Poisson distribution, we use as an error on the counts \sqrt{N} , where N is the number of counts. For the error on the angles we consider instead a uniform distribution: considering the sensibility of the instrument, we assume $\Delta\theta = \frac{1}{\sqrt{12}}$. The error on $\cos^2(\theta)$ is then obtained by propagating the error on the angle: $\Delta\cos^2(\theta) = 2\cos(\theta)\sin(\theta)\Delta\theta$. For the angles 0° and 90° the same error of the other two is taken, since for both a null value would be obtained due to the sine or the cosine. Experimental data are collected in the **Table 7**.

Angle ($^\circ$)	$\cos^2(\theta)$	Counts	Time (s)	Rate (Hz)
0.0 ± 0.3	1.0 ± 0.2	9469 ± 97	2700	3.51 ± 0.08
30.0 ± 0.3	0.7 ± 0.2	7103 ± 84	2700	2.63 ± 0.06
60.0 ± 0.3	0.2 ± 0.2	2816 ± 53	2700	1.04 ± 0.03
90.0 ± 0.3	0.0 ± 0.2	576 ± 24	2700	0.21 ± 0.01

Table 7: Experimental data obtained during the analysis of the angular distribution of the muon component of cosmic rays.

At this point a linear fit is attempted between the counting rate measured and $\cos^2(\theta)$, looking for the best parameters for the generic shape $F(\cos^2(\theta)) = q + m\cos^2(\theta)$. The linear fit is shown in the **Figure 14**.



Parameter	Fit Result
q (Hz)	0.2 ± 0.7
m (Hz)	3 ± 1
$\chi^2/d.o.f$	$0.003/2$

Table 8: Values obtained for the linear fit
 $F(\cos^2(\theta)) = q + m\cos^2(\theta)$

Figure 14: Linear fit of the Angular distribution.

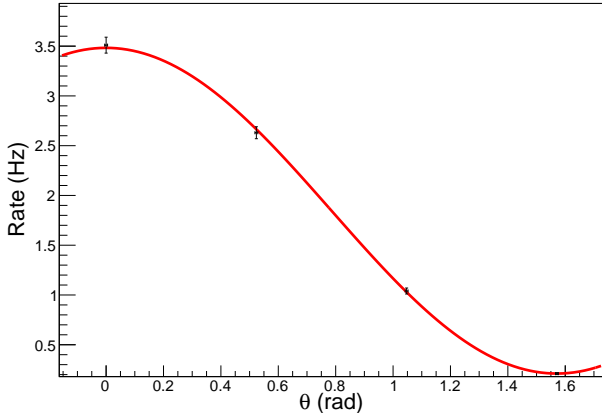


Figure 15: Cosine fit of the Angular distribution.

Since such a large uncertainty on the angle spreads expanding on the cosine, altering the confidence values of the linear fit, it is useful to verify the experimental law also by means of a fit directly between the rate of incidence and the angle, checking that the trend is a cosine square. Same results are obtained for the fit parameters, but a more reliable value of the χ^2 . The fit is shown in the **Figure 15**. The small value obtained for the χ^2 in the linear fit is probably due to the overestimation of the error on $\cos(\theta)$, while in the second fit with the angle θ a better value is obtained; anyway, in both fits the value of χ^2 indicates agreement between the experimental data and the hypothetical theoretical fit. Furthermore, it should be noted that the value of m for both fits, therefore identifiable as R_0 , is in agreement, within the error limits, with the rate obtained experimentally for the value of the angle $\theta = 0$, when $\cos(\theta) = 1$ and $R(\theta) = R_0$. The value of q , while not negligible, is still quite small. Note in fact that the width of the error on θ can affect also the fitting process, specially in the case of the linear fit. For more accurate values it would be necessary to measure at several different angles, or even to repeat the measurements for the same angle, in order to have lower errors on θ .

7 Efficiency

The experimental apparatus is constructed in such a way to minimize the energy loss of the particles that occur detect (the muons of cosmic rays) and the noise coming from environmental cosmic radiations. However, the built telescope has a limited efficiency. In particular, from the physical characteristics of the apparatus, an efficiency of 23% is expected. The last of the experiment purpose is therefore to verify the efficiency of the experimental setup in recording the events corresponding to the incidence of cosmic ray muons. To obtain this measurement, the counting rates obtained from two different experimental setups are compared: the one of the Trackers only and the one obtained by the logical AND between the two scintillators UP and DOWN and the Trackers. The efficiency is therefore given by:

$$\epsilon = \frac{UP.AND.DOWN.AND.T}{T}$$

The number of counts is taken using the 10 with 10 minute measurements. Since the number of counts N obeys to a Poisson distribution, the error on this measure is \sqrt{N} . Then the error on ϵ is obtained by propagation.

Setup	Counts
UP.AND.DOWN.AND.T	46 ± 7
T	192 ± 14

Table 10: Experimental number of counts from the CAEN scaler.

Then the telescope has an efficiency equal to:

$$\epsilon = (23 \pm 4)\%$$

in agreement with the theoretical prediction.

8 Conclusion

In conclusion, it can be said that, after having connected and calibrated the experimental apparatus, the results obtained are in excellent agreement with the theoretical predictions. In addition to the results obtained for the verification of the experimental law followed by the angular distribution of muons at Sea level further confirmation of the success of the experiment derives from the analysis of the correlation between the spectra recorded by the two detectors UP and DOWN, and from the analysis of the events collected in the edges, which precisely respect the theoretical expectations. Finally, the efficiency measurement of the experimental setup further validates the results obtained.